

# Accurate Measurement of the Electron Antineutrino Yield of U-235 Fissions from the STEREO Experiment with 119 Days of Reactor-On Data

H. Almazán,<sup>1</sup> L. Bernard,<sup>2,†</sup> A. Blanchet,<sup>3,††</sup> A. Bonhomme,<sup>1,3</sup> C. Buck,<sup>1</sup> P. del Amo Sanchez,<sup>4</sup>  
 I. El Atmani,<sup>3,†</sup> J. Haser,<sup>1</sup> L. Labit,<sup>4</sup> J. Lamblin,<sup>2</sup> A. Letourneau,<sup>3,\*</sup> D. Lhuillier,<sup>3</sup> M. Licciardi,<sup>2</sup>  
 M. Lindner,<sup>1</sup> T. Materna,<sup>3</sup> A. Onillon,<sup>3</sup> H. Pessard,<sup>4</sup> J.-S. Réal,<sup>2</sup> C. Roca,<sup>1</sup> R. Rogly,<sup>3</sup> T. Salagnac,<sup>2,††</sup>  
 V. Savu,<sup>3</sup> S. Schoppmann,<sup>1,\*\*</sup> V. Sergeyeva,<sup>4,§</sup> T. Soldner,<sup>5</sup> A. Stutz,<sup>2</sup> and M. Vialat<sup>5</sup>

(STEREO Collaboration)<sup>¶</sup>

<sup>1</sup>Max-Planck-Institut für Kernphysik, Saupfercheckweg 1, 69117 Heidelberg, Germany

<sup>2</sup>Univ. Grenoble Alpes, CNRS, Grenoble INP, LPSC-IN2P3, 38000 Grenoble, France

<sup>3</sup>IRFU, CEA, Université Paris-Saclay, 91191 Gif-sur-Yvette, France

<sup>4</sup>Univ. Grenoble Alpes, Université Savoie Mont Blanc, CNRS/IN2P3, LAPP, 74000 Annecy, France

<sup>5</sup>Institut Laue-Langevin, CS 20156, 38042 Grenoble Cedex 9, France

(Dated: April 9, 2020)

We report a measurement of the antineutrino rate from the fission of  $^{235}\text{U}$  with the STEREO detector using 119 days of reactor turned on. Considering several corrections, which are presented in detail, we achieve accurate results and report the most precise single measurement at reactors with highly enriched  $^{235}\text{U}$  fuel. We measure an IBD cross-section per fission of  $\sigma_f = (6.34 \pm 0.06 [\text{stat}] \pm 0.15 [\text{sys}] \pm 0.15 [\text{model}]) \cdot 10^{-43} \text{cm}^2/\text{fission}$  and observe a rate deficit of  $(5.2 \pm 0.8 [\text{stat}] \pm 2.3 [\text{sys}] \pm 2.3 [\text{model}])\%$  compared to the model. Here, the first and second uncertainties are experimental and the third is from the model. We confirm the deficit between the world average and the model.

PACS numbers: 14.60.Lm, 14.60.Pq, 14.60.St, 28.41.-i

Keywords: Neutrino Flux, Nuclear Reactor, Sterile Neutrinos, Uranium

In recent years, neutrino physics at nuclear reactors has entered a precision era. The neutrino mixing angle  $\theta_{13}$  was determined and constraints of the absolute antineutrino rate were achieved [1, 2]. Experiments at reactors with highly and lowly enriched  $^{235}\text{U}$  fuel [2–5] confirm the  $\sim 6\%$  deficit of observed electron antineutrinos when compared to state-of-the-art antineutrino energy spectrum calculations, known as the Reactor Antineutrino Anomaly (RAA) [6, 7]. The anomaly has triggered numerous works to find explanations. The existence of a sterile neutrino state is explored by several short baseline experiments [8–11]. The STEREO experiment is one of them searching for a non-standard oscillation in the propagation of the electron antineutrino at  $\sim 10$  m baseline [12, 13]. The Daya Bay and RENO collaborations have reported an observation of correlation between the reactor core evolution and changes in the deficit of the reactor antineutrino flux [3, 4]. They conclude that  $^{235}\text{U}$  might be the primary contributor to the RAA. However, a contribution of  $^{239}\text{Pu}$  cannot be ruled out. Updated antineutrino spectrum predictions argue for larger model uncertainties or yield a smaller deficit [14–16].

In this context, we report a precision measurement of the electron antineutrino yield with the STEREO experiment at a reactor using highly enriched  $^{235}\text{U}$  fuel. The measurement is based on 119 days of reactor-on and 211 days of reactor-off data with a high detector stability (STEREO phase-II as defined in [13]), providing 43,400 detected antineutrino events [17–20]. The STEREO detector [21] is installed at the high flux reactor (RHF, Réacteur à Haut Flux [22, 23]) of the Institut Laue-Langevin

(ILL). The RHF operates with an  $^{235}\text{U}$  enrichment of 93% thus providing a largely pure  $^{235}\text{U}$  electron antineutrino flux. STEREO is situated below a water-filled transfer channel which mitigates cosmic-induced radiations. The compactness of the fuel element (81 cm high, 41 cm in diameter) is an advantage to reduce the effect of the source volume in the calculation of the solid angle.

The STEREO detector consists of a Target volume (TG) filled with organic liquid scintillator loaded with gadolinium (Gd). It is surrounded by a Gamma-Catcher (GC) filled with unloaded liquid scintillator. The TG scintillator is composed of LAB, PXE and DIN [24]. It acts as a proton reservoir to detect electron antineutrinos via the inverse  $\beta$ -decay (IBD) reaction on hydrogen nuclei:  $\bar{\nu}_e + p \rightarrow e^+ + n$ . The TG volume is divided into 6 identical and optically separated cells. In each cell, light pulses are recorded by four 8-inch PMTs mounted above a 20 cm thick acrylic buffer. In the following, we detail the calculation of the expectation of the antineutrino rate and describe its measurement.

Since in a nuclear reactor, electron antineutrinos are produced by  $\beta^-$ -decays of fission fragments in the reactor core, their total number over one cycle can be written in good approximation as

$$N_\nu^{\text{emi}} = \frac{\langle P_{\text{th}} \rangle}{\langle E_f \rangle} \iint \sum_i [f_i(t) S_i(E_\nu)] dE_\nu dt + N_{\text{SNF}} \quad (1)$$

where  $\langle P_{\text{th}} \rangle$  is the mean reactor thermal power from nuclear reactions,  $\langle E_f \rangle$  the mean energy released per fission,  $f_i(t)$  the activity per fission of the  $i^{\text{th}}$   $\beta$ -emitter,  $S_i(E_\nu)$

the associated antineutrino energy spectrum, and  $N_{\text{SNF}}$  the contribution of the spent nuclear fuel.

The first term in Equation 1 expresses the number of fissions. It is based on the assumption that all the energy produced in one fission is converted into heat in the installation and integrally measured. By simulating the RHF in high detail using the MCNPX-2.5 [25] and TRIPOLI-4® [26] codes, we find the amount of energy loss by escaping neutrons and  $\gamma$ -rays negligible. We can thus use the total thermal power  $P_{\text{th,tot}}$  measured by the RHF and subtract the mechanical power of the water flow  $P_{\text{pumps}}$  dissipated inside the moderator tank

$$P_{\text{th}} = P_{\text{th,tot}} - P_{\text{pumps}} \quad (2)$$

with  $P_{\text{pumps}} = (0.7 \pm 0.1)$  MW [27]. The computation of the total thermal power is based on the general equation

$$P_{\text{th,tot}} = \sum_c [q_v \cdot (\rho(T_d) \cdot C_p(T_d) \cdot T_d - \rho(T_u) \cdot C_p(T_u) \cdot T_u)] \quad (3)$$

where  $q_v$  is the volumic flow rate,  $\rho$  is the volumic density of the water,  $C_p$  the calorific capacity and  $T$  the temperature. The indices  $u$  and  $d$  denote quantities measured upstream and downstream the moderator tank, respectively. The sum runs over 4 instrumented circuits  $c$  of fluids, of which the primary heavy water circuit carries 96 % of the total power. The main flow rate measurement is based on the Venturi effect induced by a calibrated diaphragm inserted in the primary circuit. All temperature and pressure sensors are duplicated for cross-monitoring and they are accurately calibrated every two years. Propagating all uncertainties leads to a 1.44 % relative accuracy [28] with a mean power during reactor-on periods used in this analysis of  $\langle P_{\text{th,tot}} \rangle = (49.9 \pm 0.7)$  MW. A significant contribution to the total relative uncertainty (0.9 %) comes from the calibration of the diaphragm, performed in the 1970's with a scale 1 mock-up of the primary circuit [29]. In the lack of evidence of any aging effects, we are assuming that the accuracy of this calibration still holds. A dedicated inspection of the diaphragm during a long reactor shutdown is under investigation.

The mean energy released per fission  $\langle E_f \rangle$  is a key ingredient to extract the number of fissions from the measured thermal power. Precise values were obtained by Ma et al. [30] using the mass conservation method proposed by Kopeikin et al. [31], where the energy release per fission is written as

$$E_f = E_{\text{tot}} - \langle E_\nu \rangle - \Delta E_{\beta\gamma} + E_{\text{nc}} \quad (4)$$

and is based on  $E_{\text{tot}}$ , the mass excess difference between the initial and the final fragmented systems after all fragments have decayed. Corrections are applied to take into account the energy loss by antineutrinos  $\langle E_\nu \rangle$ , the fraction of energy not released in the reactor due to long-lived fragments  $\Delta E_{\beta\gamma}$ , and the energy

added due to radiative neutron captures on structural elements  $E_{\text{nc}}$ . All the terms depend on the irradiation conditions. In Ma's work, the two latter terms were evaluated for a fuel irradiation time corresponding to the mid-point of a standard cycle of a pressurised water reactor (about 1.5 years cycle duration giving  $\Delta E_{\beta\gamma} = (0.35 \pm 0.02)$  MeV for  $^{235}\text{U}$ ) and for a wide range of reactor materials ( $E_{\text{nc}} = (8.57 \pm 0.22)$  MeV). We recalculated these two values for our experimental conditions of irradiation period (50 days), and of dominance of aluminium as structural material in the core and moderator tank. Using recent databases (JEFF-3.3 [32], GEFY-6.2 [33], and NUBASE2016 [34]) and a precise TRIPOLI-4® simulation of the RHF (to model the activation of structural materials) [13], we evaluated these quantities to be  $\Delta E_{\beta\gamma} = (0.6 \pm 0.1)$  MeV and  $E_{\text{nc}} = (10.3 \pm 0.2)$  MeV. The recent nuclear databases were also used to calculate an updated mass excess for the fission products of  $^{235}\text{U}$ . The obtained mean value using the cumulative fission yields from JEFF-3.3 and GEFY-6.2 amounts to  $(-173.15 \pm 0.07)$  MeV. This value has to be compared with  $(-173.86 \pm 0.06)$  MeV from Ma's work using the cumulative fission yields from JEFF-3.1 [35] and mass excesses from AME2003 [36] nuclear databases. This difference has to be considered as a bias on Ma's value. We note that the energy loss by antineutrinos requires extrapolations to energies below 2 MeV. In that region, the accumulation of long lived isotopes produced by the  $\beta$ -decay of fission fragments or neutron captures modifies the antineutrino energy spectrum compared to the instantaneous one. For that reason, the extrapolation using exponential functions fitted on the energy spectrum above 2 MeV and measured after a few hours, as done in Ma's method, may not be a good estimate for the shape. A full simulation with all  $\beta$ -decays involved in the reactor core assuming a correct modelling of the shapes of all  $\beta$ -branches is required, but unreliable at present. In the near future, progress in the summation method may refine Ma's evaluation. The relative distortion of the antineutrino energy spectrum as a function of time, due to accumulation of long-lived isotopes and transmutations by neutron captures, were calculated with the FISPACT-II code coupled to the BESTIOLE code [37]. The averaged correction over on cycle amounts to 490 keV and we use a value of  $\langle E_\nu \rangle = (9.55 \pm 0.13)$  MeV for  $^{235}\text{U}$ , the uncertainty covering the different reactor operations. In the following, and to be compatible with the previous work, we used Ma's values except for  $\langle E_\nu \rangle$ ,  $\Delta E_{\beta\gamma}$  and  $E_{\text{nc}}$ , which are specific to our irradiation conditions. Likewise, the corresponding values for  $^{239}\text{Pu}$  were updated. The contribution of  $^{239}\text{Pu}$  was calculated using the FISPACT-II evolution code [38]. It was found to be 1.4 % by the end of a nominal cycle, resulting in a mean contribution of only 0.7 % [13]. By using this weighting, the mean energy released per fission amounts to  $\langle E_f \rangle = (203.41 \pm 0.26)$  MeV.

The Huber spectrum for pure  $^{235}\text{U}$  [39] is used as a model of the second integral in Equation 1. As the Huber model is defined in the [2, 8] MeV range, we restrict our analysis to this energy range. The model is corrected for the fission fraction of  $^{239}\text{Pu}$ , the time-evolution of fission fragment activities, and activation of structural elements [13]. The fraction of  $^{239}\text{Pu}$  reduces the averaged antineutrino rate over one cycle by less than 0.3%. For the energy range of our analysis, it is found to affect mainly the three lowest 500 keV-wide energy bins above 2.4 MeV antineutrino energy. The maximum contribution of less than 2% is found in the first bin. The activation of structural materials was inferred using the TRIPOLI-4® simulation of the RHF. It was found that mainly  $^{28}\text{Al}$  and  $^{56}\text{Mn}$  contribute. Combining all low energy corrections leads to a sizeable increase of the total rate of emitted antineutrinos by  $(7.2 \pm 0.4)\%$  with respect to the Huber model [13, 40]. Because of the lower IBD cross-section at low antineutrino energy, the impact on the predicted number of detected antineutrinos per fission is smaller, about  $(1.6 \pm 0.1)\%$  neglecting experimental thresholds and cut efficiencies. The extra uncertainty is negligible compared to the initial uncertainty of 2.4% of the Huber model (see Table I). Finally, the term  $N_{\text{SNF}}$  in Equation 1 arises from spent fuel elements stored in the transfer channel above the STEREO detector. It was estimated with FISPACT-II coupled to BESTIOLE to be less than 0.1% after 24 h of a reactor stop, justifying that in our analysis only data after this time are considered. The remaining effect is further suppressed in the analysis by the subtraction of reactor-on and -off data.

From the total number of emitted antineutrinos, the predicted number of detected antineutrinos can be written as

$$N_{\nu}^{\text{pred}} = N_{\nu}^{\text{emi}} \cdot \tau_{\text{int}} \cdot c_p^{\text{Data/MC}} \cdot \epsilon_{\text{d}} \cdot c_n^{\text{Data/MC}} \quad (5)$$

with the fraction of interacting antineutrinos  $\tau_{\text{int}}$ , the proton number correction  $c_p^{\text{Data/MC}}$ , the total detection efficiency  $\epsilon_{\text{d}}$ , and the correction of the detection efficiency of the delayed signal  $c_n^{\text{Data/MC}}$ . All these quantities are tabulated in Table I and discussed in the following.

The fraction of antineutrinos which interact in the detector can be written as

$$\tau_{\text{int}} = \iiint S(E_{\nu}) \sigma_{\text{IBD}}(E_{\nu}) \frac{\rho_f(\vec{r}_c) \rho_H(\vec{r}_d)}{4\pi |\vec{r}_d - \vec{r}_c|^2} d\vec{r}_d d\vec{r}_c dE_{\nu} \quad (6)$$

where  $S(E_{\nu})$  is the antineutrino energy spectrum normalised by integral to unity,  $\sigma_{\text{IBD}}(E_{\nu})$  is the IBD cross-section [41],  $\vec{r}_c$  and  $\vec{r}_d$  are the coordinates of the antineutrino emission and interaction vertices,  $\rho_f(\vec{r}_c)$  is the fission density distribution in the core, normalised to unity and inferred from the MCNPX-2.5 simulation, and  $\rho_H(\vec{r}_d)$  is the hydrogen density in the fiducial volume of the detector. This integral is numerically computed using a Monte-Carlo (MC) method including the description of

TABLE I. Summary of all relevant quantities and their corresponding relative uncertainties on the IBD yield.

Quantity	Symbol	Value	Uncert./%
Number of $\nu$ /fission	$N_{\nu}^{[2,8]\text{MeV}}$	1.846	2.40
Huber prediction		1.722	2.40
Correction factors		1.072	0.10
Number of fissions/day		$1.30 \cdot 10^{23}$	1.44
Thermal power	$\langle P_{\text{th}} \rangle$	49.2 MW	1.44
Energy/fission	$\langle E_f \rangle$	203.4 MeV	0.13
Fract. of interacting $\nu$	$\tau_{\text{int}}$	$8.10 \cdot 10^{-21}$	0.56
Solid angle			0.50
IBD cross-section	$\sigma_{\text{IBD}}$		0.22
MC statistics			0.12
Correc. of $p$ -number	$c_p^{\text{Data/MC}}$	0.983	1.00
Detection efficiency	$\epsilon_{\text{d}}$	0.2049	0.54
Selection cuts			0.41
Energy Scale			0.30
MC statistics			0.19
Correc. of delayed effi.	$c_n^{\text{Data/MC}}$	0.9774	0.86
Predicted IBD yield		$383.7 \text{ d}^{-1}$	$2.10 \oplus 2.40$
Observed IBD yield		$363.8 \text{ d}^{-1}$	$0.88 \oplus 1.06$
Statistics			0.88
$\nu$ extrac. method			0.65
Reactor-induced bkg.			0.83
Off-time method			0.14

the reactor and detector setups. The emission vertices are generated randomly within the core following the fission density distribution. Likewise, also the interaction vertices are generated randomly within a portion of a hollow sphere enclosing the STEREO detector and following a  $1/|\vec{r}_d - \vec{r}_c|^2$  distribution. The fraction of interactions  $\tau_{\text{int}}$  has been found to be  $(8.10 \pm 0.05) \cdot 10^{-21}$ . The uncertainty on  $\tau_{\text{int}}$  includes the geometrical solid angle uncertainty (0.50%), the IBD cross-section uncertainty (0.22%), and a statistical uncertainty (0.12%) of the MC [21]. It does not include the Huber model uncertainty. The factor  $c_p^{\text{Data/MC}} = (0.983 \pm 0.010)$  corrects the number of hydrogen atoms used in the MC model to the one measured during detector filling [13, 24].

In the experiment, IBD-candidates are identified as two successive events within a time coincidence window of [2, 70]  $\mu\text{s}$ , passing energy cuts. These energy cuts are set to select the positron candidate (prompt signal) in the [1.625, 7.125] MeV energy range and the neutron candidate (delayed signal) in the [4.5, 10.0] MeV energy range. In addition to these basic selection cuts, a muon veto and topological selections are used to improve the accidental and correlated backgrounds rejections [13]. All these rejection cuts induce detection inefficiencies that are calculated and propagated into the prediction.

The total detection efficiency  $\epsilon_{\text{d}}$  is computed using GEANT4 [42, 43] and FIFRELIN [44–46] simulations, as well as the same antineutrino generator as for the estimation of the fraction of interacting antineutrinos [13]. This term describes, for the antineutrinos of [2, 8] MeV ki-

netic energy which interact in the scintillator or acrylics, the fraction passing all selection cuts. It evaluates the global acceptance efficiency of the prompt and delayed signals due to selection cuts, the fraction of neutron captures by Gd compared to other nuclei (mainly hydrogen) in the TG, and the amount of events (either neutrons or  $\gamma$ -rays from the capture process) escaping to other volumes free of Gd. For the distribution of vertices obtained in the MC simulations, the total detection efficiency amounts to  $\epsilon_d = (0.2049 \pm 0.0011)$ . Even if the MC has been extensively checked and tuned with a variety of calibration  $\gamma$ -sources, some corrections still have to be applied to correctly reproduce the neutron physics inside the detector. These corrections were evaluated using an AmBe  $\gamma$ -neutron source in the experiment and in the simulation. The correction factor between data and MC for the delayed signal amounts to  $C_n^{\text{Data/MC}} = (0.9774 \pm 0.0084)$  [47].

Finally, the predicted antineutrino rate yields to  $(383.7 \pm 8.1 [\text{sys}] \pm 9.2 [\text{model}]) \bar{\nu}_e/\text{day}$ , where the experimental and Huber model uncertainties were separated as the latter is common to all experiments. The experimental antineutrino rate is extracted by a fit to the distributions of the pulse shape (PSD) of IBD-candidates measured during reactor-on and reactor-off periods [13]. Integrated over 119 days of reactor-on periods and 211 days of reactor-off periods, the IBD rate amounts to  $(363.8 \pm 5.0) \bar{\nu}_e/\text{day}$ . The uncertainty is due to statistics (0.88%), an added systematic uncertainty including systematic effects in the PSD fit and covering small discrepancies when extracting the IBD rate with the method described in [48] (0.65%, corresponding to half of the discrepancy), another systematic uncertainty to cover the contribution of a possible reactor-induced background (0.83%) [13], and a systematic uncertainty to cover any potential bias in the off-time extraction method of accidental coincidences (0.14%) [13].

The comparison with the prediction gives an observed to predicted ratio of  $0.948 \pm 0.008 [\text{stat}] \pm 0.023 [\text{sys}] \pm 0.023 [\text{model}]$ , where the first uncertainty is statistical, the second combines all experimental systematic uncertainties listed in Table I, and the third uncertainty is from the Huber model, common to all experiments. All systematic uncertainties are treated uncorrelated. Considering only the two experimental uncertainties, we find very good agreement with the world average of pure  $^{235}\text{U}$  measurements [2]. Our measurement confirms the deviation from the Huber model as shown in Figure 1. Including our measurement, the world average is improved from  $(0.950 \pm 0.015)$  to  $(0.950 \pm 0.013)$ , where again only experimental uncertainties are considered.

To determine the IBD cross-section per fission, we use an extrapolated Huber spectrum  $S_H(E_\nu)$  for pure  $^{235}\text{U}$  without corrections for  $^{28}\text{Al}$ ,  $^{56}\text{Mn}$ , and off-equilibrium

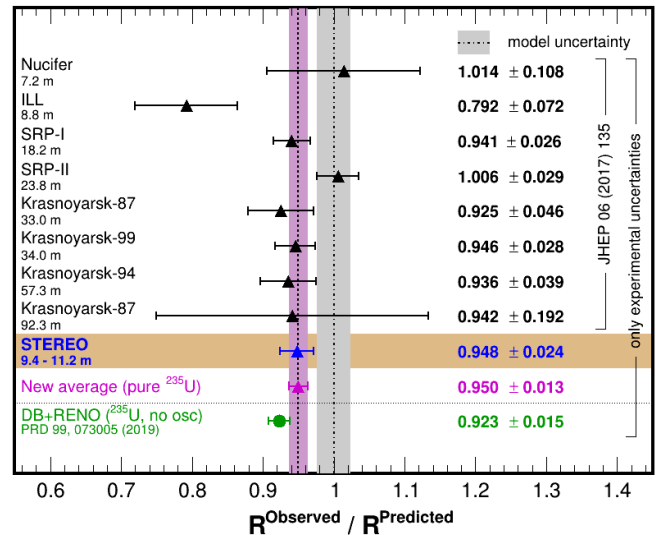


FIG. 1. Ratios between measured antineutrino yields and the Huber model predictions of various experiments. The uncertainty bars represent only experimental uncertainties. The common model uncertainty of 2.4% is shown as grey band around unity. Values of other experiments are taken from [2, 50, and references therein]. For Daya Bay and RENO we show only the ratio for the  $^{235}\text{U}$  component. The value is taken from a fit, where isotopic IBD yields of  $^{235}\text{U}$  and  $^{239}\text{Pu}$  are free, while those of  $^{238}\text{U}$  and  $^{241}\text{Pu}$  are constrained to the prediction [50].

effects. The corresponding integral

$$\sigma_f = \int_{1.8 \text{ MeV}}^{10.0 \text{ MeV}} S_H(E_\nu) \sigma_{\text{IBD}}(E_\nu) dE_\nu \quad (7)$$

yields a predicted theoretical value of  $(6.69 \pm 0.15) \cdot 10^{-43} \text{cm}^2/\text{fission}$  [49]. Applying our observed to predicted ratio, we get  $\sigma_f = (6.34 \pm 0.06 [\text{stat}] \pm 0.15 [\text{sys}] \pm 0.15 [\text{model}]) \cdot 10^{-43} \text{cm}^2/\text{fission}$ , confirming the value in [50].

The result presented in this letter demonstrates the ability of the STEREO experiment to achieve an accurate measurement of the electron antineutrino rate coming from a pure  $^{235}\text{U}$  fuel element. It confirms the observed deficit from the Huber model corresponding to the RAA and is in agreement with the measured world-average. While our result is already the most precise among all pure  $^{235}\text{U}$  measurements, further improvement is possible as additional data taking is in progress. Until the end of 2020, a two-fold increase of the dataset is expected.

We thank the ILL divisions DRe and DPT for their help in the precise determination of the reactor power and solid angle. Moreover, we are grateful for the technical and administrative support of the ILL for the installation and operation of the STEREO detector. This work is funded by the French National Research Agency



(ANR) within the project ANR-13-BS05-0007 and the “Investments for the future” programmes P2IO LabEx (ANR-10-LABX-0038) and ENIGMASS LabEx (ANR-11-LABX-0012). We further acknowledge the support of the CEA, in particular the financial support of the Cross-Disciplinary Programme on Numerical Simulation of CEA, the CNRS/IN2P3 and the Max Planck Society.

- 
- <sup>†</sup> Present address: Ecole Polytechnique, CNRS/IN2P3, Laboratoire Leprince-Ringuet, 91128 Palaiseau, France
- <sup>††</sup> Present address: LPNHE, Sorbonne Université, Université de Paris, CNRS/IN2P3, 75005 Paris, France
- <sup>‡</sup> Present address: Hassan II University, Faculty of Sciences, Aïn Chock, BP 5366 Maarif, Casablanca 20100, Morocco
- <sup>\*</sup> [alain.letourneau@cea.fr](mailto:alain.letourneau@cea.fr)
- <sup>‡‡</sup> Present address: Institut de Physique Nucléaire de Lyon, CNRS/IN2P3, Univ. Lyon, Université Lyon 1, 69622 Villeurbanne, France
- <sup>\*\*</sup> [stefan.schoppmann@mpi-hd.mpg.de](mailto:stefan.schoppmann@mpi-hd.mpg.de)
- <sup>§</sup> Present address: Institut de Physique Nucléaire Orsay, CNRS/IN2P3, 15 rue Georges Clemenceau, 91406 Orsay, France
- <sup>¶</sup> <http://www.stereo-experiment.org>
- [1] I. Esteban, M.C. Gonzalez-Garcia, A. Hernandez-Cabezudo, M. Maltoni, and T. Schwetz, Global analysis of three-flavour neutrino oscillations: synergies and tensions in the determination of  $\theta_{23}$ ,  $\delta_{CP}$ , and the mass ordering, *Journal of High Energy Physics* **2019**, 106 (2019), [arXiv:1811.05487 \[hep-ph\]](https://arxiv.org/abs/1811.05487).
- [2] S. Gariazzo, C. Giunti, M. Laveder, and Y. Li, Updated global 3+1 analysis of short-baseline neutrino oscillations, *Journal of High Energy Physics* **2017**, 135 (2017), [arXiv:1703.00860 \[hep-ph\]](https://arxiv.org/abs/1703.00860).
- [3] D. Adey *et al.*, Improved measurement of the reactor antineutrino flux at Daya Bay, *Physical Review D* **100** (2019), [arXiv:1808.10836 \[hep-ex\]](https://arxiv.org/abs/1808.10836).
- [4] G. Bak *et al.* (RENO Collaboration), Fuel-composition dependent reactor antineutrino yield at RENO, *Physical Review Letters* **122** (2019), [arXiv:1806.00574 \[hep-ex\]](https://arxiv.org/abs/1806.00574).
- [5] H. de Kerret *et al.* (Double Chooz Collaboration), First Double Chooz  $\theta_{13}$  measurement via total neutron capture detection (2019), [arXiv:1901.09445 \[hep-ex\]](https://arxiv.org/abs/1901.09445).
- [6] T.A. Mueller *et al.*, Improved predictions of reactor antineutrino spectra, *Phys. Rev. C* **83**, 054615 (2011), [arXiv:1101.2663 \[hep-ex\]](https://arxiv.org/abs/1101.2663).
- [7] G. Mention *et al.*, Reactor antineutrino anomaly, *Phys. Rev. D* **83**, 073006 (2011), [arXiv:1101.2755 \[hep-ex\]](https://arxiv.org/abs/1101.2755).
- [8] I. Alekseev *et al.*, Search for sterile neutrinos at the DANSS experiment, *Physics Letters B* **787**, 56 (2018), [arXiv:1804.04046 \[hep-ex\]](https://arxiv.org/abs/1804.04046).
- [9] Y.J. Ko *et al.* (NEOS Collaboration), Sterile neutrino search at the NEOS experiment, *Phys. Rev. Lett.* **118**, 121802 (2017), [arXiv:1610.05134 \[hep-ex\]](https://arxiv.org/abs/1610.05134).
- [10] J. Ashenfelter *et al.* (PROSPECT Collaboration), First search for short-baseline neutrino oscillations at HFIR with PROSPECT, *Phys. Rev. Lett.* **121**, 251802 (2018), [arXiv:1806.02784 \[hep-ex\]](https://arxiv.org/abs/1806.02784).
- [11] A.P. Serebrov *et al.*, The first observation of ef-

- fect of oscillation in Neutrino-4 experiment on search for sterile neutrino, *JETP Letters* **109**, 213 (2019), [arXiv:1809.10561 \[hep-ex\]](https://arxiv.org/abs/1809.10561).
- [12] H. Almazán *et al.* (STEREO Collaboration), Sterile neutrino constraints from the STEREO experiment with 66 days of reactor-on data, *Phys. Rev. Lett.* **121**, 161801 (2018), [arXiv:1806.02096 \[hep-ex\]](https://arxiv.org/abs/1806.02096).
- [13] H. Almazán *et al.*, Improved sterile neutrino constraints from the STEREO experiment with 179 days of reactor-on data (2019), [arXiv:1912.06582 \[hep-ex\]](https://arxiv.org/abs/1912.06582).
- [14] A.C. Hayes, J.L. Friar, G.T. Garvey, G. Jungman, and G. Jonkmans, Systematic uncertainties in the analysis of the reactor neutrino anomaly, *Phys. Rev. Lett.* **112**, 202501 (2014), [arXiv:1309.4146 \[nucl-th\]](https://arxiv.org/abs/1309.4146).
- [15] A.C. Hayes and P. Vogel, Reactor neutrino spectra, *Annual Review of Nuclear and Particle Science* **66**, 219 (2016), [arXiv:1605.02047 \[hep-ph\]](https://arxiv.org/abs/1605.02047).
- [16] M. Estienne *et al.*, Updated summation model: An improved agreement with the Daya Bay antineutrino fluxes, *Physical Review Letters* **123** (2019), [arXiv:1904.09358 \[nucl-ex\]](https://arxiv.org/abs/1904.09358).
- [17] D. Lhuillier *et al.* (STEREO Collaboration), *STEREO run - cycle 181* (2018).
- [18] D. Lhuillier *et al.* (STEREO Collaboration), *STEREO run cycle 2018/02* (2018).
- [19] D. Lhuillier *et al.* (STEREO Collaboration), *STEREO run - cycle 184* (2018).
- [20] D. Lhuillier *et al.* (STEREO Collaboration), *STEREO run shutdown 2018-19* (2018).
- [21] N. Allemandou *et al.*, The STEREO experiment, *Journal of Instrumentation* **13** (07), P07009, [arXiv:1804.09052 \[physics.ins-det\]](https://arxiv.org/abs/1804.09052).
- [22] *Rapport Transparence et Sécurité Nucléaire du Réacteur Haut Flux*, Tech. Rep. (Institut Laue-Langevin, 2018).
- [23] G. Campioni *et al.*, A critical experiment at HFR of 19 March 2008, *Annals of Nuclear Energy* **36**, 1319 (2009).
- [24] C. Buck, B. Gramlich, M. Lindner, C. Roca, and S. Schoppmann, Production and properties of the liquid scintillators used in the STEREO reactor neutrino experiment, *Journal of Instrumentation* **14** (01), P01027, [arXiv:1812.02998 \[physics.ins-det\]](https://arxiv.org/abs/1812.02998).
- [25] <http://mcnp.lanl.gov>.
- [26] E. Brun *et al.*, TRIPOLI-4®, CEA, EDF and AREVA reference Monte Carlo code, *Annals of Nuclear Energy* **82**, 151 (2015).
- [27] *Rapport de Sûreté INB n° 67 – Réacteur à Haut Flux*, Tech. Rep. (Institut Laue-Langevin, 2017).
- [28] C.-E. Fillion, *Détermination de la puissance du réacteur de l'ILL pour la prédiction du flux de neutrinos*, Internship report (CEA Paris Saclay, 2017) rapport de stage.
- [29] G. Muller and K. Nowak, *Étalonnage du diaphragme de mesure du réacteur à haut flux Grenoble*, Tech. Rep. (1990) appendices 1 and 3 of the ILL technical letter DRe/mc-90/074, Rapport n° 44.01.10.
- [30] X.B. Ma, W.L. Zhong, L.Z. Wang, Y.X. Chen, and J. Cao, Improved calculation of the energy release in neutron-induced fission, *Phys. Rev. C* **88**, 014605 (2013).
- [31] V.I. Kopeikin, L.A. Mikaelyan, and V.V. Sinev, Reactor as a source of antineutrinos: Thermal fission energy, *Physics of Atomic Nuclei* **67**, 1892 (2004), [arXiv:hep-ph/0410100 \[hep-ph\]](https://arxiv.org/abs/hep-ph/0410100).
- [32] <http://www.oecd-nea.org/dbdata/jeff/jeff33> (2018).
- [33] <http://www.oecd-nea.org/janisweb/tree/n/gefy-6.2>.
- [34] G. Audi, F.G. Kondev, M. Wang, W.J. Huang, and S.

- Naimi, The NUBASE2016 evaluation of nuclear properties, *Chinese Physics C* **41**, 030001 (2017).
- [35] <http://www.oecd-nea.org/dbdata/jeff/> (2016).
- [36] G. Audi, A.H. Wapstra, and C. Thibault, The Ame2003 atomic mass evaluation: (II) Tables, graphs and references, *Nuclear Physics A* **729**, 337 (2003), the 2003 NUBASE and Atomic Mass Evaluations.
- [37] T. Mueller, *Expérience Double Chooz: simulation des spectres antineutrinos issus de réacteurs*, Ph.D. thesis, Université de Paris-Sud (2010).
- [38] J.-Ch. Sublet *et al.*, FISPACT-II: An advanced simulation system for activation, transmutation and material modelling, *Nuclear Data Sheets* **139**, 77 (2017).
- [39] P. Huber, On the determination of anti-neutrino spectra from nuclear reactors, *Phys. Rev. C* **84**, 024617 (2011), [Erratum: *Phys. Rev. C* **85**, 029901 (2012)], [arXiv:1106.0687](https://arxiv.org/abs/1106.0687) [hep-ph].
- [40] I. El Atmani, Search for eV neutrino sterile: Status of STEREO experiment (2020), *J. Phys.: Conf. Ser.* submitted, [arXiv:2002.12701](https://arxiv.org/abs/2002.12701) [hep-ex].
- [41] A. Strumia and F. Vissani, Precise quasielastic neutrino/nucleon cross-section, *Physics Letters B* **564**, 42–54 (2003), [arXiv:astro-ph/0302055](https://arxiv.org/abs/hep-ph/0302055) [astro-ph].
- [42] J. Allison *et al.*, Recent developments in Geant4, *Nucl. Instrum. Meth. A* **835**, 186 (2016).
- [43] S. Agostinelli *et al.*, Geant4 - a simulation toolkit, *Nucl. Instrum. Meth. A* **506**, 250 (2003).
- [44] O. Litaize, O. Serot, and L. Berge, Fission modelling with FIFRELIN, *Eur. Phys. J. A* **51**, 177 (2015).
- [45] H. Almazán *et al.*, Improved STEREO simulation with a new gamma ray spectrum of excited gadolinium isotopes using FIFRELIN, *Eur. Phys. J. A* **55**, 183 (2019), [arXiv:1905.11967](https://arxiv.org/abs/1905.11967) [physics.ins-det].
- [46] H. Almazán *et al.*, Data from: Improved STEREO simulation with a new gamma ray spectrum of excited gadolinium isotopes using FIFRELIN, *Zenodo* **2653786** (2019).
- [47] H. Almazán, *Evaluation of the neutron detection efficiency in the STEREO reactor neutrino experiment*, Ph.D. thesis, Ruperto-Carola-University, Heidelberg (2020).
- [48] H. Almazán *et al.* (STEREO Collaboration), Search for light sterile neutrinos with the STEREO experiment, *European Physical Journal Web of Conferences* **219**, 08001 (2019), [arXiv:1804.09052](https://arxiv.org/abs/1804.09052) [physics.ins-det].
- [49] F.P. An *et al.* (Daya Bay Collaboration), Evolution of the reactor antineutrino flux and spectrum at Daya Bay, *Phys. Rev. Lett.* **118**, 251801 (2017), [arXiv:1704.01082](https://arxiv.org/abs/1704.01082) [hep-ex].
- [50] C. Giunti, Y.F. Li, B.R. Littlejohn, and P.T. Surukuchi, Diagnosing the reactor antineutrino anomaly with global antineutrino flux data, *Physical Review D* **99** (2019), [arXiv:1901.01807](https://arxiv.org/abs/1901.01807) [hep-ph].